Abdominal Radiology

Published online: 8 September 2018

Abdom Radiol (2019) 44:529–538
https://doi.org/10.1007/s00261-018-1766-y

Differentiation of hepatic abscess from metastasis on contrast-enhanced dynamic computed tomography in patients with a history of extrahepatic malignancy: emphasis on dynamic change of arterial rim enhancement

Jae Gu Oh,[1] Seo-Youn Choi,[1] Min Hee Lee,[1] Ji Eun Lee,[1] Boem Ha Yi,[1] Seung Soo Kim,[2] Ji Hye Min,[3] and Bora Lee[4]

[1]Department of Radiology, Bucheon Hospital, Soonchunhyang University College of Medicine, 170 Jomaru-ro, Bucheon 14584, Korea
[2]Department of Radiology, Cheonan Hospital, Soonchunhyang University College of Medicine, Cheonan, Korea
[3]Department of Radiology, Chungnam National University Hospital, Chungnam National University College of Medicine, Daejeon, Korea
[4]Department of Biostatistics, Graduate School of Chung-Ang University, Seoul, Korea

Abstract

Objectives: The objective of the study is to identify computed tomography (CT) findings that differentiate hepatic abscess from hepatic metastasis in a patient with a history of extrahepatic malignancy.
Materials and methods: This retrospective study included 30 patients with 93 hepatic abscesses and 40 patients with 125 hepatic metastases who had a history of extrahepatic malignancy and underwent contrast-enhanced dynamic CT with arterial phase (AP) and portal venous phase (PVP). The diagnosis of hepatic abscess and hepatic metastasis was made using pathological confirmation or clinical diagnosis. Margin, patchy parenchymal enhancement, arterial rim enhancement, dynamic change of arterial rim enhancement, size discrepancy of lesions between arterial and portal phases, bile duct dilatation, perilesional hyperemia, and perilesional low density were evaluated by two radiologists independently. Significant findings for differentiating two groups were identified at univariate and multivariate analysis with nomogram for predicting hepatic abscess. Interobserver agreement was also analyzed for each variable.
Results: Multivariate analysis revealed that patchy parenchymal enhancement ($P < 0.001$), arterial rim enhancement persistent through PVP ($P < 0.001$), and perilesional hyperemia ($P = 0.013$) were independent significant findings to predict hepatic abscess than metastasis. Among them, arterial rim enhancement persistent through PVP showed a highest odds ratio (OR 33.73) on multivariate analysis and a highest predictor point on a nomogram for predicting hepatic abscess. When two of these three criteria were combined, 80.7% (75/93) of hepatic abscess were correctly identified, with a specificity of 85.6% (107/125). When all three criteria were satisfied, specificity was up to 100% (125/125).
Conclusions: At contrast-enhanced dynamic CT, patchy parenchymal enhancement, arterial rim enhancement persistent through PVP, perilesional hyperemia, and their combinations may be reliable CT features for differentiating hepatic abscess from metastasis in patients with a history of primary extrahepatic malignancy.

Key words: Liver abscess—Metastasis—Computed tomography

Abbreviations

CT	Computed tomography
AP	Arterial phase
PVP	Portal venous phase

Electronic supplementary material The online version of this article (https://doi.org/10.1007/s00261-018-1766-y) contains supplementary material, which is available to authorized users.

Correspondence to: Seo-Youn Choi; *email:* sychoi@schmc.ac.kr

MRI	Magnetic resonance imaging
HBPI	Hepatobiliary phase image
TP	Transitional phase

Hepatic metastasis is the most common malignant lesion of the liver and is even more common than primary hepatic tumors [1]. Characteristic imaging findings of hepatic metastasis have been reported, including rim enhancement, centripetal enhancement, and capsular retraction adjacent to a mass [2]. On the other hand, hepatic abscess is a localized collection of necrotic inflammatory materials from a bacterial, fungal, or parasitic infection [3] and its characteristic imaging findings are ''double target sign'' and ''cluster sign'' [4–6].

Although the treatment strategy of these two diseases is completely different, differentiating hepatic abscess from hepatic metastasis by imaging is still challenging to the radiologists [7]. Even though several studies have attempted to identify the imaging features that differentiate hepatic abscess and metastasis [8–10], all of these studies have evaluated magnetic resonance imaging (MRI) findings to find out the differential points. To our knowledge, there has been only one paper dealing with comparison of computed tomography (CT) finding between hepatic abscess and metastasis [11]. However, they included a single case of abscess in a non-metastasis group for comparison with hepatic metastasis. Thus, this study could not provide the accurate differential point between two groups.

Peripheral rim enhancement has been known to be a non-specific imaging finding that can be observed in various benign and malignant lesions including hepatic metastasis and abscess [10–13]. Although several studies have shown interest in whether rim enhancement is seen or not in metastasis, only a few studies discussed the dynamic change of the rim enhancement to differentiate hepatic abscess from metastasis using MRI [10, 14, 15]. Among them, one recent study [10] found that persistent rim enhancement through transitional phase (TP) on gadoxetic acid-enhanced MRI suggested hepatic microabscess, whereas disappearance or absence of arterial rim enhancement on TP imaging indicated hepatic metastasis. Similar results were reported by Balci et al. [15] and Choi et al. [14]: Arterial rim enhancement of abscesses was enhanced on hepatobiliary phase image (HBPI). This finding is referred to as non-defect of arterial enhancing rim on HBPI. However, the results from these studies were derived from MRI findings and focused on the changes in arterial enhanced rim through transitional or hepatobiliary phases on MRI using hepatocyte-specific contrast. Therefore, it is not appropriate to apply this finding to the contrast-enhanced CT. However, to the best of our knowledge, no studies exist on dynamic changes in rim enhancement on CT as a diagnostic feature for hepatic abscess.

Thus, the purpose of this study was to investigate the imaging findings of hepatic abscess on contrast-enhanced CT to differentiate from hepatic metastasis and to assess the value of a dynamic change of rim enhancement on CT for differentiating hepatic abscess from metastasis.

Materials and methods

Patient population

Our institutional review board approved this study and waived the requirements to obtain informed consent because of the retrospective nature of clinical and imaging data collection. Between January 2012 and April 2017, we searched our radiologic database for patients who had underlying primary extrahepatic malignancy and underwent contrast-enhanced abdomen CT with the terms ''abscess'' or ''metastasis'' of the liver on radiologic reports.

We found 60 patients with hepatic abscess and 57 patients with hepatic metastasis. Of these 117 patients, 47 were excluded for absence of either arterial phase or portal phase ($n = 21$), loss of follow-up without pathological confirmation or clinical diagnosis of abscess or metastasis ($n = 15$), lesions such as cyst or hemangioma other than abscess or metastasis identified by MRI ($n = 8$), or poor image quality for interpretation ($n = 3$). Thus, data on 30 patients with hepatic abscess (13 males and 17 females, mean age 68.2 years; age range 45–83 years) and 40 patients with hepatic metastasis (20 males and 20 females, mean age 61.5 years; age range 37–87 years) were analyzed. Among the 30 patients in the abscess group, 4 were pathologically diagnosed by biopsy, and the others were clinically diagnosed. Clinical diagnosis of hepatic abscess was performed when lesions disappeared or decreased in size with antibiotic treatment on follow-up CT or MRI. The 30 patients with hepatic abscess had a total of 93 hepatic abscesses as follows: 9 patients had only one lesion, 7 patients had two or three, 3 patients had four, and the remaining 11 patients had five or more. The most common underlying primary extrahepatic malignancy was pancreatic cancer ($n = 11$), followed by extrahepatic bile duct cancer ($n = 8$), ampulla of Vater cancer ($n = 7$), gall bladder ($n = 3$), and breast ($n = 1$). In contrast, among the 40 patients in the metastasis group, 28 were pathologically diagnosed by surgery ($n = 17$) or biopsy ($n = 11$), and the others were clinically diagnosed. Clinical diagnosis of hepatic metastasis was based on development of new focal hepatic lesions or increased size on follow-up CT or MRI and responding to chemotherapy. A total of 125 metastases were identified in the 40 patients as follows: 9

patients had solitary metastasis, 11 patients had two metastases, 4 patients had three or four, and 16 patients had 5 or more metastatic lesions. The most common underlying primary extrahepatic malignancy was colorectal cancer (n = 16), followed by pancreatic cancer (n = 9), extrahepatic bile duct cancer (n = 4), breast cancer (n = 3), lung cancer (n = 2), Ampulla of Vater cancer (n = 1), gallbladder cancer (n = 1), renal cell carcinoma (n = 1), nasopharyngeal carcinoma (n = 1), small bowel gastrointestinal stromal tumor (GIST) (n = 1), and stomach GIST (n = 1) (Fig. 1). The abscess group showed a significantly higher proportion (13/30; 43.3%) of elevated total bilirubin (normal range < 1.2 mg/dL) than the metastasis group (7/40; 17.5%) (P = 0.036). Laboratory data at the time of CT examinations are shown in supplementary Table 1.

CT examination

All scans were obtained using three commercially available multi-detector CT (MDCT) scanners (Scope, and Definition Flash, Siemens, Forchheim, Germany; Discovery CT750 HD, GE Medical Systems, Milwaukee, WI, USA). Axial scans were acquired at a section thickness of 3 mm with a 3-mm reconstruction interval, field of view of 300–370 mm, gantry rotation time of 0.5 s, tube current-time product of 110–140 mA, and peak voltage of 100–130 kVp. For 16-, 64-, and 128-detector CT examinations, detector collimations were 0.75, 0.625, and 0.5 mm with table speeds of 13.5, 12.0, and 46.8 mm per rotation, respectively. Coronal reformatted images were obtained based on axial images with 3-mm section thickness.

Unenhanced and contrast-enhanced CT scans were performed with full inspiration during short breath-holds. Non-ionic contrast medium (Iohexol, Bonorex 350; Central Medical Service, Seoul, Korea) was administered at 3.0 mL/s with an automatic dual-headed power injector (OptiVantage DH, Mallinckrodt, St Louis, MO, USA) into 18- or 20-gage intravenous cannula (2 ml/kg body weight). An arterial phase scan was obtained 20 s after a bolus-tracking trigger setting of CT value 100 Hounsfield units (HU) of the thoracic aorta. Portal venous phase (PVP) was acquired 55 s after arterial phase scanning.

Image analysis

All CT images were reviewed by two radiologists (OOO and OOO; 2 and 9 years of experience in abdominal CT imaging interpretation, respectively) independently on a picture archiving and communication system (PACS). Both readers were aware of the alternative diagnoses of hepatic abscess or metastasis. However, they were blinded whether each lesion belonged to either the abscess or metastasis group and blinded to clinical information and histopathological results. After the first independent image analysis, interobserver agreement was assessed for evaluated CT imaging parameters. Then, the two reviewers met to make final decisions by consensus for each discordant case.

We evaluated qualitative imaging parameters of (a) multiplicity (single or multiple, two or more lesions), (b) margin (well defined or fuzzy, evaluated at the tumor periphery on axial AP and PVP), (c) patchy parenchymal enhancement (patchy or geographic enhancement throughout the liver on AP [16]), (d) bile duct dilatation, (e) perilesional hyperemia (fuzzy-marginated hyperenhancement outside the tumor border on AP that became

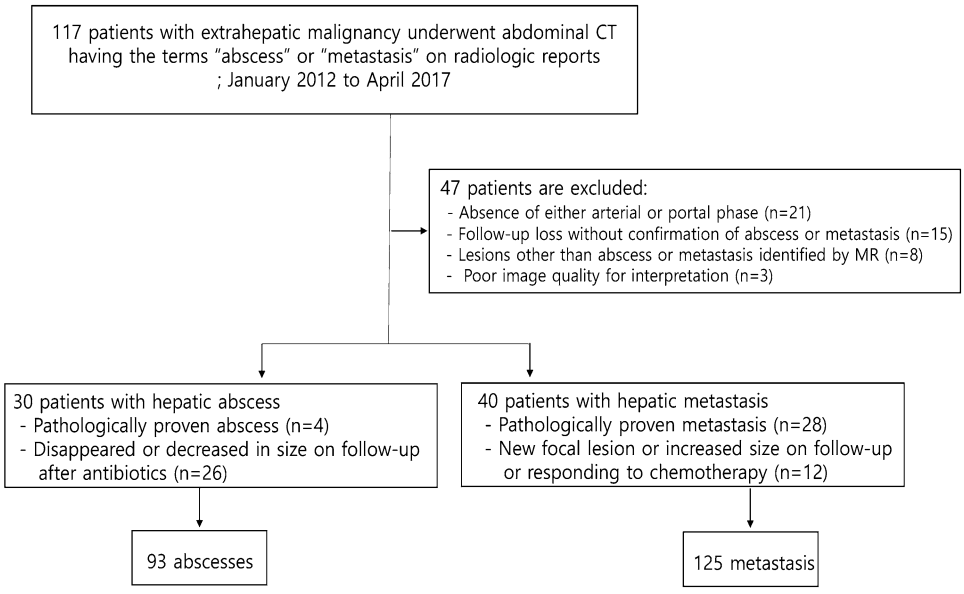

Fig. 1. Flow chart of inclusion and exclusion criteria.

isodense with normal liver parenchyma in PVP [17, 18]), (f) perilesional low density on PVP (indicating edema of the surrounding normal hepatic parenchyma [4]), (g) significant size discrepancy of the lesion between arterial and portal venous phases (decreased longest diameter ≥ 30% on PVP) [19, 20]), (h) arterial rim enhancement, and (i) dynamic change of arterial rim enhancement (arterial rim enhancement persistent through PVP, arterial rim enhancement disappeared through PVP, or no rim on any phase). In order to reduce the confusion between arterial rim enhancement and perilesional hyperemia, arterial rim enhancement was limited to ring-like area with hyperenhancement along the periphery of central hypodense area in arterial phase, with thickness of 3 mm or less. Otherwise, it was defined as perilesional hyperemia when surrounding hyperenhancement was greater than 3 mm in thickness and fuzzy outer margin.

The lesion size was measured with longest transverse diameter of each lesion (in centimeters) measured in the axial plane on each phase. When measuring the size of the lesion with rim enhancement, the size was measured up to the outer margin including rim enhancement.

Statistical analysis

The χ^2 or Fisher's exact test compared categorical variables for differentiating between two groups (sex, multiplicity, margin, perilesional hyperemia, patchy parenchymal enhancement, bile duct dilatation, perilesional low density, size discrepancy between arterial and portal venous phases, arterial rim enhancement, and dynamic change of arterial rim enhancement). Student's *t* test was performed for continuous variables (age and size). To differentiate two diseases, stepwise logistic regression was used to make a multivariable regression model based on Akaike Information Criteria and select significant variables. Nomogram was constructed on the basis of this prediction model. Interobserver agreement was determined for each variable using Kappa statistics. Conventional interpretation was poor agreement, < 0.20; fair, 0.20–039; moderate, 0.40–0.59; substantial, 0.60–0.79; and almost perfect, 0.80.

All statistical analysis was performed using statistical software (SPSS version 17, SPSS, Chicago, IL; and R version 3.3.2, R Foundation for Statistical Computing, Vienna, Austria). Significant differences were defined as $P < 0.05$.

Results

Demographic characteristics

Baseline demographic characteristics of patients are demonstrated in Table 1. No significant demographic differences were observed between the two groups in sex or multiplicity of lesions ($P > 0.05$). In contrast, patients with hepatic abscess were significantly older than those with hepatic metastasis (68.2 ± 10.3 years vs. 61.5 ± 12.0 years).

CT imaging characteristics

The results of qualitative analysis are summarized in Table 1. In univariate analysis, hepatic abscess more frequently showed well-defined margin on PVP ($P < 0.001$), patchy parenchymal enhancement ($P < 0.001$), size discrepancy of the lesion between AP and PVP ($P < 0.001$), bile duct dilatation ($P < 0.001$), perilesional hyperemia ($P < 0.001$), and perilesional low density on PVP ($P < 0.001$). Arterial rim enhancement was more frequently seen in hepatic abscess than hepatic metastasis as well ($P < 0.001$). Given the changes of rim enhancement through arterial to portal venous phases, arterial rim that was persistent through PVP was more frequent in hepatic abscess, whereas hepatic metastasis more frequently showed that arterial rim disappeared on PVP and there was no enhanced rim on any phase ($P < 0.001$). At quantitative analysis, the lesion size of hepatic abscess was significantly smaller than that of hepatic metastasis [1.6 cm ± 1.1 (range 0.5–7.8 cm) vs. 2.9 cm ± 2.0 (range 0.7–8.0 cm), respectively; $P < 0.001$].

In multivariate analysis (Table 2), patchy parenchymal enhancement ($P < 0.001$), arterial rim enhancement persistent through PVP ($P < 0.001$), and perilesional hyperemia ($P < 0.001$) were revealed as significant variables for predicting hepatic abscess rather than hepatic metastasis. A regression coefficient-based nomogram was constructed from the significant variables (Fig. 2). Sensitivity, specificity, accuracy, positive likelihood ratio (LR+), and negative likelihood ratio (LR−) for significant imaging findings and their combinations are demonstrated in Table 3 and supplementary Table 2. When two of the three criteria were combined, 807% (95% CI 71.2–88.1%) of hepatic abscesses were identified with a specificity of 85.6% (95% CI 78.2–91.2%). When all three criteria were satisfied, specificity was 100.0% (95% CI 97.1–100.0%) (Figs. 3, 4, 5). Interobserver agreement for all imaging findings was substantial to perfect (k = 0.64–0.86).

Discussion

Our study demonstrated that, among various CT findings, patchy parenchymal enhancement, arterial rim enhancement persistent through PVP, and perilesional hyperemia were significant independent variables for predicting hepatic abscess than metastasis. Combining two of these criteria resulted in specificity of 85.6%. Combining all three criteria resulted in specificity maximized to 100.0%, which could be considered reliable for predicting hepatic abscess. In addition, we presented a

Table 1. Characteristics and univariable analysis of hepatic abscess and metastasis on contrast-enhanced CT

Variables	Abscess $N = 30$	Metastasis $N = 40$	Total $N = 70$	P value	K value
By patient					
Age	68.2 ± 10.3	61.5 ± 12.0	64.3 ± 11.7	0.017	
Sex					
Male	13 (43.3%)	20 (50.0%)	33 (47.1%)	0.756	
Female	17 (56.7%)	20 (50.0%)	37 (52.9%)		
Multiplicity					
Single	9 (30.0%)	9 (22.5%)	18 (25.7%)	0.664	
Multiple	21 (70.0%)	31 (77.5%)	52 (74.3%)		
Variables	Abscess $N = 93$	Metastasis $N = 125$	Total $N = 218$	P value	K value
By lesion					
Size	1.6 ± 1.1	2.9 ± 2.0	2.4 ± 1.8	< 0.001	
Margin on AP					
Well defined	39 (41.9%)	54 (43.2%)	93 (42.7%)	0.852	0.75
Fuzzy	54 (58.1%)	71 (56.8%)	125 (57.3%)		
Margin on PVP					
Well defined	85 (91.4%)	85 (68.0%)	170 (78.0%)	< 0.001	0.76
Fuzzy	8 (8.6%)	40 (32.0%)	48 (22%)		
Patchy parenchymal enhancement					
Presence	75 (80.6%)	31 (24.8%)	106 (48.6%)	< 0.001	0.84
Absence	18 (19.4%)	94 (75.2%)	112 (51.4%)		
Arterial rim enhancement					
Presence	81 (87.1%)	57 (45.6%)	138 (63.3%)	< 0.001	0.86
Absence	12 (12.9%)	68 (54.4%)	80 (36.7%)		
Dynamic change of arterial rim enhancement					
Arterial rim enhancement persistent through PVP	68 (73.1%)	22 (17.6%)	90 (41.3%)	< 0.001	0.78
Arterial rim enhancement disappeared on PVP	13 (14.0%)	35 (28.0%)	48 (22.0%)		
No rim on any phase	12 (12.9%)	68 (54.4%)	80 (36.7%)		
Size discrepancy between AP and PVP					
Presence	42 (45.2%)	21 (16.8%)	63 (28.9%)	< 0.001	0.77
Absence	51 (54.8%)	104 (83.2%)	155 (71.1%)		
Bile duct dilatation					
Presence	60 (64.5%)	10 (8.0%)	70 (32.1%)	< 0.001	0.86
Absence	33 (35.5%)	115 (92.0%)	148 (67.9%)		
Perilesional hyperemia					
Presence	70 (75.3%)	39 (31.2%)	109 (50.0%)	< 0.001	0.66
Absence	23 (24.7%)	86 (68.8%)	109 (50.0%)		
Perilesional low density on PVP					
Presence	14 (15.1%)	0 (0.0%)	14 (6.4%)	0.986	0.64
Absence	79 (84.9%)	125 (100%)	204 (93.6%)		

AP, arterial phase, PVP, portal venous phase

nomogram for individualized risk estimation that calculates the numerical probability of hepatic abscess.

In our study, all imaging findings related to rim enhancement, namely, rim enhancement on AP and dynamic change of arterial rim enhancement were significantly different between hepatic abscess and metastasis ($P < 0.05$). However, of these findings, arterial rim enhancement persistent through PVP was only the independent significant variable related to rim enhancement for predicting hepatic abscess. Further, among all significant variables, arterial rim enhancement persistent through PVP showed a highest odds ratio (33.73) on multivariate analysis and a highest predictor point on a nomogram for predicting hepatic abscess. Whereas the presence of rim enhancement is considered a characteristic sign of hepatic abscess, it is a well-known finding that can also be seen in malignancies, especially hepatic metastasis. It has been reported that rim enhancement in hepatic abscesses is reported to correspond to the granulation tissue of the abscesses [21], and that of hepatic metastasis is associated with the viable tumors in tumor periphery [22–24]. A previous study using gadoxetic acid-enhanced MRI by Choi et al. [10] also found that arterial rim enhancement that was persistent through the transitional phase of liver dynamic MRI indicated hepatic abscess over metastasis. They hypothesized that the fibro-inflammatory process with vascular-rich granulation tissue in the periphery of the abscess, where hepatocyte function begins to recover, is responsible for persistent rim enhancement [10]. Although our study revealed that rim enhancement on AP was a significant predictor for hepatic abscess over metastasis ($P < 0.001$ in univariate analysis), we observed this feature in about half (45.6%) of the metastasis group and considered it as a less specific

Table 2. Univariate and multivariate analyses for distinguishing abscess from metastasis

Variable	Univariate		Multivariate	
	OR (95% CI)	*P* value	OR (95% CI)	*P* value
Margin on AP				
Well defined	0.95(0.55, 1.63)	0.852		
Fuzzy	1 (Ref.)			
Margin on PVP				
Well defined	5.00 (2.32, 12.09)	< 0.001		
Fuzzy	1 (Ref.)			
Patchy parenchymal enhancement				
Presence	12.63 (6.69, 24.92)	< 0.001	32.82 (11.1, 141.14)	< 0.001
Absence	1 (Ref.)		1 (Ref.)	
Arterial rim enhancement				
Presence	8.05 (4.12, 16.89)	< 0.001		
Absence	1 (Ref.)			
Dynamic change of arterial rim enhancement				
Arterial rim enhancement persistent through PVP	12.73 (6.77, 24.91)	< 0.001	33.73 (11.35, 145.49)	< 0.001
Arterial rim enhancement disappeared on PVP or no rim on any phase	1 (Ref.)		1 (Ref.)	
Size discrepancy between AP and PVP				
Presence	4.08 (2.21, 7.71)	< 0.001		
Absence	1 (Ref.)			
Bile duct dilatation				
Presence	20.91 (10.03, 47.62)	< 0.001		
Absence	1 (Ref.)			
Perilesional hyperemia				
Presence	6.71 (3.72, 12.48)	< 0.001	2.77 (1.24, 6.29)	0.013
Absence	1 (Ref.)		1 (Ref.)	
Perilesional low density on PVP				
Presence	67317741.05 (0.00, NA)	0.986		
Absence	1 (Ref.)			

AP, arterial phase; PVP, portal venous phase

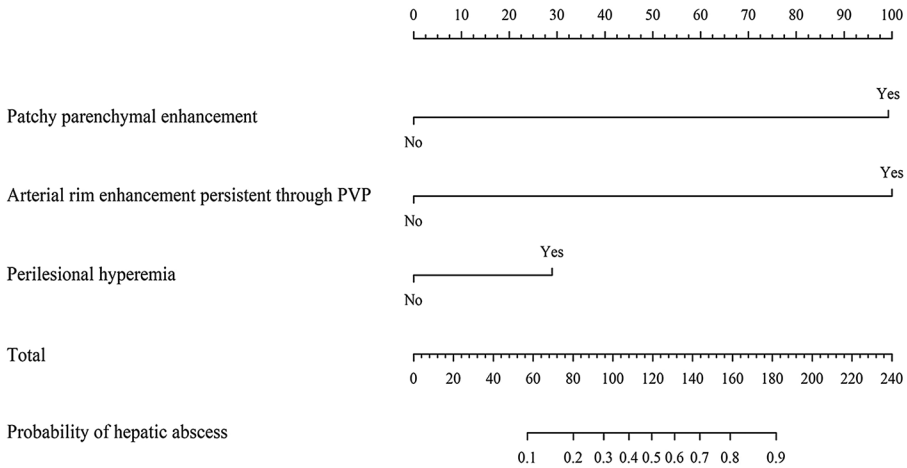

Fig. 2. Nomogram for predicting the probability of hepatic abscess than hepatic metastasis. Top: predictor points are found on uppermost point scale that corresponds to each variable. Bottom: points for all variables are added and translated into probability of hepatic abscess. Patchy parenchymal enhancement: 1, Arterial rim enhancement persistent through PVP: 1, perilesional hyperemia: 1.

finding. Considering that arterial rim enhancement persistent through PVP is an independent finding and had high specificity (82.4%), it could be more important as a differential point for predicting hepatic abscess.

Several studies have reported that perilesional hyperemia is one of the imaging features that can be associated with hepatic abscess, derived from decreased localized portal flow caused by acute inflammation of the hepatic parenchyma surrounding the abscess and compensatory arterial flow increase [4, 25]. Toshifumi et al. [26] suggested this to differentiate hepatic abscesses from metastases. Similar to previous studies, our study also demonstrated that perilesional hyperemia was an independent significant finding for hepatic abscess.

Table 3. Diagnostic performance of four significant imaging findings and combinations for predicting hepatic abscess

Combination	Value of diagnostic performance % (95% CI)				
	Sensitivity	Specificity	Accuracy	LR +	LR−
Patchy parenchymal enhancement	75/93 80.7 (71.2–88.1)	94/125 75.2 (66.7–82.5)	169/218 77.5 (71.4–82.9)	3.25 (2.36–4.48)	0.26 (0.17–0.39)
Arterial rim enhancement persistent through PVP	68/93 73.1 (62.9—81.8)	103/125 82.4(74.6–88.6)	171/218 78.4 (72.4–83.7)	4.15 (2.79–6.19)	0.33 (0.23–0.46)
Perilesional hyperemia	70/93 75.3 (65.2–83.6)	86/125 68.8 (59.9–76.8)	156/218 71.6 (65.1–77.5)	2.41 (1.81–3.21)	0.36 (0.25–0.52)
Any two	75/93 80.7 (71.2–88.1)	107/125 85.6 (78.2–91.2)	95/125 83.5 (77.9–88.2)	5.60 (3.61–8.69)	0.23 (0.15–0.34)
All three	47/93 50.5 (40.0–61.1)	125/125 100 (97.1–100.0)	172/218 78.9 (72.9–84.1)	–	0.49 (0.40–0.61)

Data in parentheses are 95% confidence interval
As the specificity of all three combinations is 100%, LR + in all three combinations cannot be calculated with a formula
CI, confidence interval; LR+, positive likelihood ratio; LR−, negative likelihood ratio; AP, arterial phase; PVP, portal venous phase

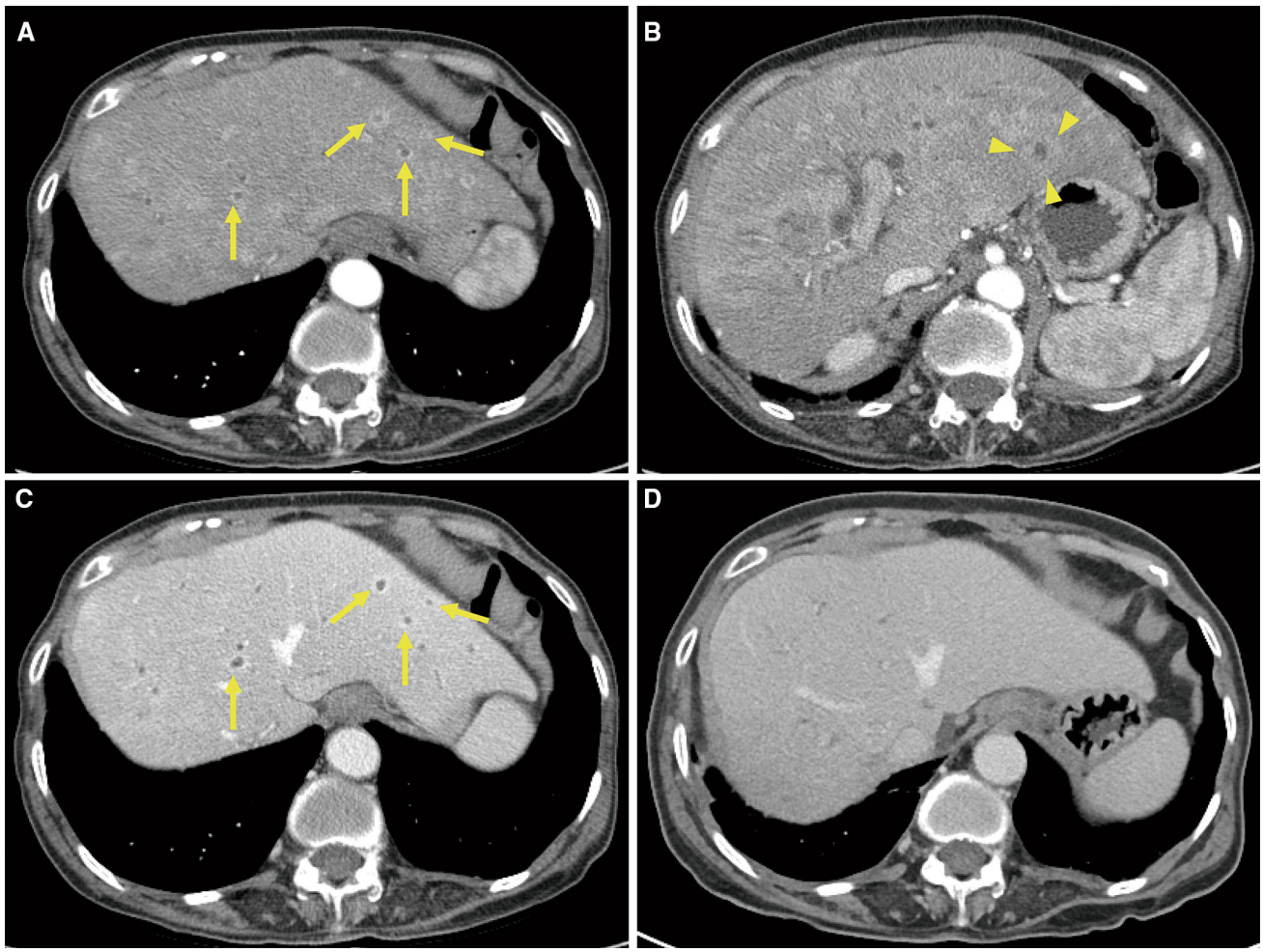

Fig. 3. A 70-year-old woman with extrahepatic bile duct cancer(cholangiocarcinoma) and multiple hepatic abscesses. Dynamic contrast-enhanced CT with multiple hepatic lesions in both hepatic lobes with fuzzy outer margin and clear inner margin. Arterial phase imaging **A**, **B** shows patchy parenchymal enhancement of the liver and perilesional hyperemia (arrowheads). Intrahepatic biliary dilatation was noted due to underlying hilar cholangiocarcinoma. Portal venous phase imaging **C** shows persistent rim enhancement (arrows in C) from arterial phase (arrows in a). These features were regarded as hepatic abscesses and disappeared in follow-up CT **D** with antibiotic treatment alone during follow-up.

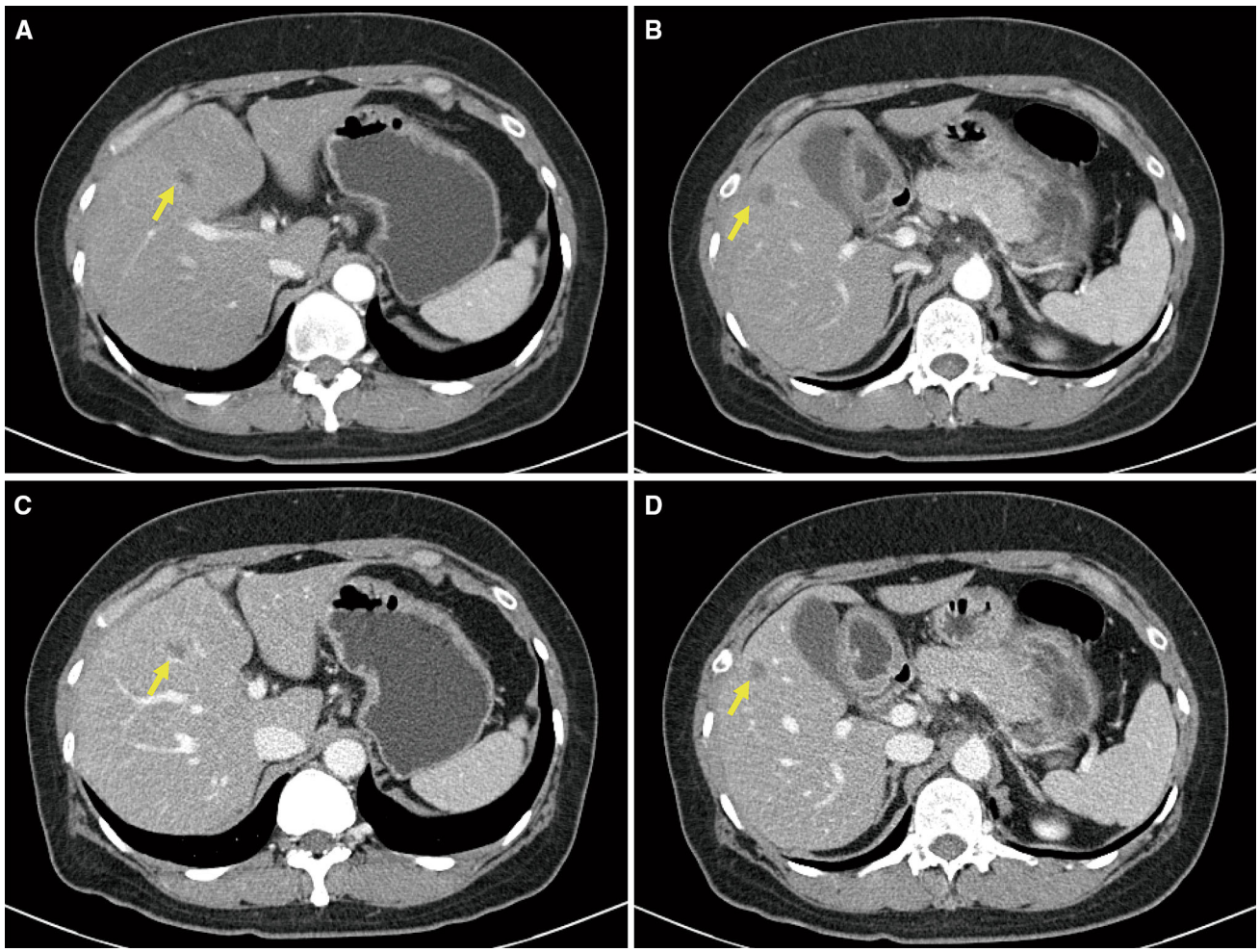

Fig. 4. A 46-year-old woman with colon cancer and hepatic metastasis. Dynamic contrast-enhanced CT with two hepatic lesions in segments IV (arrow in A) and V (arrow in B) (**A**, **B**). Patchy parenchymal enhancement and perilesional hyperemia were not observed on arterial phase image. Arterial (**A**, **B**) and portal (**C**, **D**) phase images showed no rim enhancement. Features were diagnosed as hepatic metastasis via surgical resection.

Various conditions have been recognized as reasons for focal or segmental hepatic parenchymal enhancement, including arterioportal shunt, portal vein compression or thrombosis, aberrant blood supply, steal effect, hepatic venous outflow obstruction or thrombosis, and biliary obstruction with or without cholangitis [24, 27]. Therefore, focal or segmental hepatic parenchymal enhancement is considered a non-specific finding that can be associated with various diseases rather than being specific to a particular disease including hepatic abscess. Our study, however, found that patchy parenchymal enhancement of the liver was an independently significant finding for discriminating between hepatic abscess and metastasis. Whereas 24.8% (31/125) of hepatic metastases showed patchy parenchymal enhancement of the liver, 80.6% (75/93) of hepatic abscesses had this feature. Although specificity was relatively low (69%, 86/125) compared with other independent findings, we expect that patchy parenchymal enhancement could be supportive in differentiating hepatic abscess from metastasis. Further, when combined with arterial rim enhancement persistent through PVP, specificity increased to 100%.

Dual-energy CT has been admitted to reflect the increased blood vessels of the lesion and it can be expressed more easily by using color-corded iodine-specific and virtual monochromatic images. [28–32]. All of the patchy parenchymal enhancement, arterial rim enhancement persistent through PVP, and perilesional hyperemia, which were significant imaging findings suggesting hepatic abscess in this study, are considered to the features related to increased blood flow by inflammation. Considering this, we expect that diagnostic performance of CT for prediction of hepatic abscess could be improved with dual-energy CT.

Our study had several limitations. Firstly, it was limited by the retrospective review of select patient groups, so there was an inevitable selection bias. Because we included all patients with underlying history of

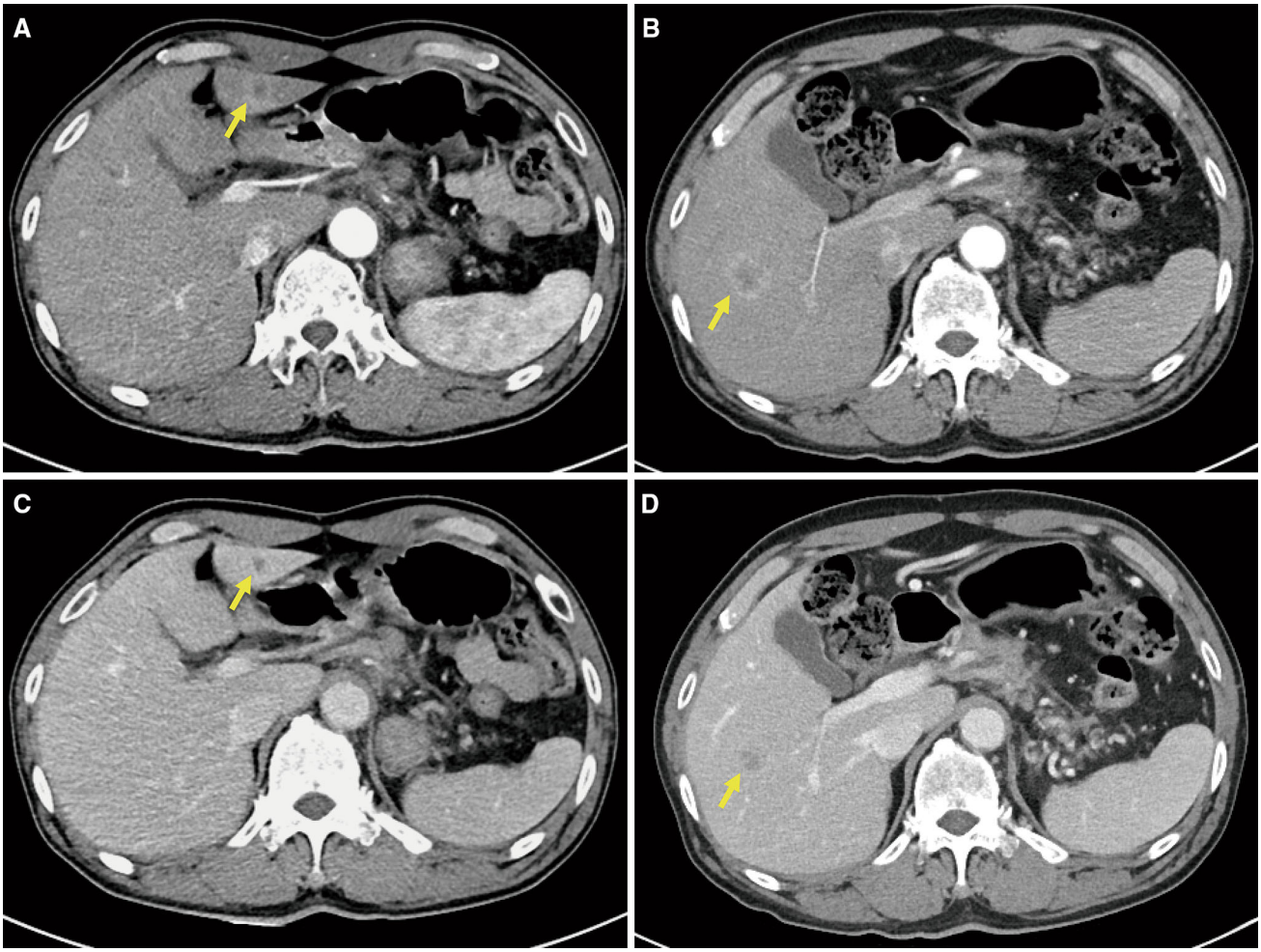

Fig. 5. A 56-year-old man with pancreatic tail cancer and hepatic metastasis. Dynamic contrast-enhanced CT with two hepatic lesions in segments III and V with fuzzy outer margin and unclear inner margin (**A**, **B**). Patchy parenchymal enhancement and perilesional hyperemia were not observed on arterial phase image. Arterial phase imaging (**A**, **B**) shows arterial rim enhancement that disappeared on portal phase image (**C**, **D**). The lesions were diagnosed as hepatic metastasis via biopsy using transabdominal ultrasound.

malignancy, our results might not be applied to all patients without underlying malignancy. Secondly, histological proof was not obtained for some included lesions. However, in cases without pathologic confirmation, we included only strongly suspected abscesses and metastases according to our criteria. Thirdly, an external analysis was not performed using an independent validation set to validate the ratios used to construct the nomogram. Thus, these values need to be verified through a larger prospective study in the future. Fourthly, we did not consider the size cut-off (lower or upper limits) when selecting the patients. Because larger lesion could show more obvious image features on CT, the results might not be applied to smaller lesions. Although size itself could affect the multivariate analysis as an independent variable, the number of smaller lesions ($n = 54$) was much smaller when setting the size cut of 1 cm than larger lesions ($n = 164$) in this study. So we suggested that the effects of size could be minimized than expected. Lastly, the subgroup analysis was not performed using patients with biliary or pancreatic malignancies. The differentiation of hepatic abscess from hepatic metastasis is more challenging especially in the patients with biliary or pancreatic malignancies because these conditions were prone to develop both hepatic abscess and hepatic metastasis. However, in this study, the number of the patients with biliary or pancreatic malignancies was so small that we could not perform subgroup analysis.

In summary, dynamic contrast-enhanced CT could be helpful for differentiating hepatic abscess from metastasis in patients with a history of primary extrahepatic malignancy. Among CT imaging findings, patchy parenchymal enhancement, arterial rim enhancement persistent through PVP, and perilesional hyperemia were significant independent variables for predicting hepatic abscess.

Compliance with ethical standards

Funding This work was supported by the National Research Foundation of Korea (NRF) grant funded by the Korea government (MSIT) (No. 2018R1C1B5030985). This work was supported by the Soonchunhyang University Research Fund.

Conflict of interest J.G.O. declares that he has no conflict of interest. S.Y.C. declares that she has no conflict of interest. H.K.L. declares that she has no conflict of interest. M.H.L. declares that she has noconflict of interest. J.E.L. declares that she has no conflict of interest. B.H.Y. declares that she has no conflict of interest. S.S.K. declares that he has no conflict of interest. J.H.M. declares that she has no conflict of interest. B.L. declares that she has no conflict of interest.

Ethical approval All procedures performed in studies involving human participants were in accordance with the ethical standards of the institutional and/or national research committee and with the 1964 Helsinki declaration and its later amendments or comparable ethical standards. Informed consent was waived for retrospective nature of clinical and imaging data collection in this study.

References

1. Imam K, Bluemke DA (2000) MR imaging in the evaluation of hepatic metastases. Magn Reson Imaging Clin N Am 8(4):741–756
2. Sica GT, Ji H, Ros PR (2000) CT and MR imaging of hepatic metastases. Am J Roentgenol 174(3):691–698. https://doi.org/10.2214/ajr.174.3.1740691
3. Krige JEJ, Beckingham IJ (2001) Liver abscesses and hydatid disease. BMJ 322(7285):537–540
4. Mathieu D, Vasile N, Fagniez PL, et al. (1985) Dynamic CT features of hepatic abscesses. Radiology 154(3):749–752. https://doi.org/10.1148/radiology.154.3.3969480
5. Jeffrey RB Jr, Tolentino CS, Chang FC, Federle MP (1988) CT of small pyogenic hepatic abscesses: the cluster sign. AJR Am J Roentgenol 151(3):487–489. https://doi.org/10.2214/ajr.151.3.487
6. Vilgrain V, Esvan M, Ronot M, et al. (2016) A meta-analysis of diffusion-weighted and gadoxetic acid-enhanced MR imaging for the detection of liver metastases. Eur Radiol 26(12):4595–4615. https://doi.org/10.1007/s00330-016-4250-5
7. Bachler P, Baladron MJ, Menias C, et al. (2016) Multimodality imaging of liver infections: differential diagnosis and potential pitfalls. Radiographics 36(4):1001–1023. https://doi.org/10.1148/rg.2016150196
8. Méndez RJ, Schiebler ML, Outwater EK, Kressel HY (1994) Hepatic abscesses: MR imaging findings. Radiology 190(2):431–436. https://doi.org/10.1148/radiology.190.2.8284394
9. Park HJ, Kim SH, Jang KM, et al. (2013) Differentiating hepatic abscess from malignant mimickers: value of diffusion-weighted imaging with an emphasis on the periphery of the lesion. J Magn Reson Imaging 38(6):1333–1341. https://doi.org/10.1002/jmri.24112
10. Choi SY, Kim YK, Min JH, et al. (2017) The value of gadoxetic acid-enhanced MRI for differentiation between hepatic microabscesses and metastases in patients with periampullary cancer. Eur Radiol 27(10):4383–4393. https://doi.org/10.1007/s00330-017-4782-3
11. Nino-Murcia M, Olcott EW, Jeffrey RB, et al. (2000) Focal liver lesions: pattern-based classification scheme for enhancement at arterial phase CT. Radiology 215(3):746–751. https://doi.org/10.1148/radiology.215.3.r00jn03746
12. Kakkar C, Polnaya AM, Koteshwara P, et al. (2015) Hepatic tuberculosis: a multimodality imaging review. Insights Imaging 6(6):647–658. https://doi.org/10.1007/s13244-015-0440-y
13. Wooten WB, Bernardino ME, Goldstein HM (1978) Computed tomography of necrotic hepatic metastases. AJR Am J Roentgenol 131(5):839–842. https://doi.org/10.2214/ajr.131.5.839
14. Choi SH, Lee CH, Kim BH, et al. (2013) "Nondefect" of arterial enhancing rim on hepatobiliary phase in 3.0-T gadolinium-ethoxybenzyl-diethylenetriamine pentaacetic acid-enhanced liver magnetic resonance imaging: distinguishing hepatic abscess from metastasis. J Comput Assist Tomogr 37(6):849–855. https://doi.org/10.1097/RCT.10.1097/RCT.0b013e318297211a
15. Balci NC, Semelka RC, Noone TC, et al. (1999) Pyogenic hepatic abscesses: MRI findings on T1- and T2-weighted and serial gadolinium-enhanced gradient-echo images. J Magn Reson Imaging 9(2):285–290
16. Arai K, Kawai K, Kohda W, et al. (2003) Dynamic CT of acute cholangitis: early inhomogeneous enhancement of the liver. Am J Roentgenol 181(1):115–118. https://doi.org/10.2214/ajr.181.1.1810115
17. Yu J-S, Rofsky NM (2006) Hepatic metastases: perilesional enhancement on dynamic MRI. Am J Roentgenol 186(4):1051–1058. https://doi.org/10.2214/AJR.04.1698
18. Semelka RC, Hussain SM, Marcos HB, Woosley JT (2000) Perilesional enhancement of hepatic metastases: correlation between MR imaging and histopathologic findings—initial observations. Radiology 215(1):89–94. https://doi.org/10.1148/radiology.215.1.r00mr2989
19. Park MS, Kim MJ, Lim JS, et al. (2009) Metastasis versus focal eosinophilic infiltration of the liver in patients with extrahepatic abdominal cancer: an evaluation with gadobenate dimeglumine-enhanced magnetic resonance imaging. J Comput Assist Tomogr 33(1):119–124. https://doi.org/10.1097/RCT.0b013e3181641b1a
20. Lee MH, Kim SH, Kim H, Lee MW, Lee WJ (2011) Differentiating focal eosinophilic infiltration from metastasis in the liver with gadoxetic acid-enhanced magnetic resonance imaging. Korean J Radiol 12(4):439–449. https://doi.org/10.3348/kjr.2011.12.4.439
21. Qian LJ, Zhu J, Zhuang ZG, et al. (2013) Spectrum of multilocular cystic hepatic lesions: CT and MR imaging findings with pathologic correlation. Radiographics 33(5):1419–1433. https://doi.org/10.1148/rg.335125063
22. van Leeuwen MS, Noordzij J, Feldberg MA, Hennipman AH, Doornewaard H (1996) Focal liver lesions: characterization with triphasic spiral CT. Radiology 201(2):327–336. https://doi.org/10.1148/radiology.201.2.8888219
23. Honda H, Matsuura Y, Onitsuka H, et al. (1992) Differential diagnosis of hepatic tumors (hepatoma, hemangioma, and metastasis) with CT: value of two-phase incremental imaging. Am J Roentgenol 159(4):735–740. https://doi.org/10.2214/ajr.159.4.1326884
24. Lin G, Lunderquist A, Hagerstrand I, Boijsen E (1984) Postmortem examination of the blood supply and vascular pattern of small liver metastases in man. Surgery 96(3):517–526
25. Mathieu D, Vasile N, Fagniez PL, et al. (1985) Dynamic CT features of hepatic abscesses. Radiology 154(3):749–752. https://doi.org/10.1148/radiology.154.3.3969480
26. Gabata T, Kadoya M, Matsui O, et al. (2001) Dynamic CT of hepatic abscesses. Am J Roentgenol 176(3):675–679. https://doi.org/10.2214/ajr.176.3.1760675
27. Pradella S, Centi N, La Villa G, Mazza E, Colagrande S (2009) Transient hepatic attenuation difference (THAD) in biliary duct disease. Abdom Imaging 34(5):626–633. https://doi.org/10.1007/s00261-008-9445-z
28. Lv P, Lin XZ, Li J, Li W, Chen K (2011) Differentiation of small hepatic hemangioma from small hepatocellular carcinoma: recently introduced spectral CT method. Radiology 259(3):720–729. https://doi.org/10.1148/radiol.11101425
29. Yu Y, He N, Sun K, et al. (2013) Differentiating hepatocellular carcinoma from angiomyolipoma of the liver with CT spectral imaging: a preliminary study. Clin Radiol 68(9):e491–497. https://doi.org/10.1016/j.crad.2013.03.027
30. Yu Y, Lin X, Chen K, et al. (2013) Hepatocellular carcinoma and focal nodular hyperplasia of the liver: differentiation with CT spectral imaging. Eur Radiol 23(6):1660–1668. https://doi.org/10.1007/s00330-012-2747-0
31. Wang Q, Shi G, Qi X, Fan X, Wang L (2014) Quantitative analysis of the dual-energy CT virtual spectral curve for focal liver lesions characterization. Eur J Radiol 83(10):1759–1764. https://doi.org/10.1016/j.ejrad.2014.07.009
32. Kim JE, Kim HO, Bae K, et al. (2017) Differentiation of small intrahepatic mass-forming cholangiocarcinoma from small liver abscess by dual source dual-energy CT quantitative parameters. Eur J Radiol 92:145–152. https://doi.org/10.1016/j.ejrad.2017.05.012